NF

NASA Technical Memorandum 82634

New Technique for the Direct Measurement of Core Noise from Aircraft Engines

Eugene A. Krejsa
Lewis Research Center
Cleveland, Ohio

Prepared for the
Seventeenth Joint Propulsion Conference
cosponsored by the AIAA, SAE, and ASME
Colorado Springs, Colorado, July 27-29, 1981

NASA

NEW TECHNIQUE FOR THE DIRECT MEASUREMENT OF CORE NOISE FROM AIRCRAFT ENGINES

by Eugene A. Krejsa*

National Aeronautics and Space Administration
Lewis Research Center
Cleveland, Ohio 44135

Abstract

A new technique is presented for directly measuring the core noise levels from gas turbine aircraft engines. The technique requires that fluctuating pressures be measured in the far-field and at two locations within the engine core. The cross-spectra of these measurements are used to determine the levels of the far-field noise that propagated from the engine core. The technique makes it possible to measure core noise levels even when other noise sources dominate. The technique was applied to signals measured from an AVCO Lycoming YF102 turbofan engine. Core noise levels as a function of frequency and radiation angle were measured and are presented over a range of power settings.

Introduction

One of the sources of gas turbine aircraft engine noise that can be a significant contributor to the total noise of the newer, quieter gas turbine aircraft engines, is core noise. In the context of this paper, the term core noise is used to refer to that low frequency engine noise source usually considered to originate in the combustor. For example, core noise dominates the noise produced by the QCGAT engine described in reference 1. This engine was designed using the latest engine noise reduction techniques including acoustic treatment for fan noise reduction and a mixer nozzle for jet noise reduction. Analysis of data from static tests of this engine indicated that the far-field noise from this engine is dominated by low frequency core noise. The level of this core noise was determined to be about 10 dB higher than had been predicted (ref. 1).

Two commonly-used correlations for the prediction of core noise are presented in references 2 and 3. Both of these correlations are based on overall combustor parameters. However, that of reference 3 also includes a term for the attenuation through the turbine. These correlations are at best approximate and may be inapplicable to engines not similar to those used to generate the correlations. Two factors contribute to the difficulty in making core noise predictions. The first factor is that there may not be a single source of low frequency core noise. Core noise is usually considered to originate as pressure fluctuations in the combustor. A number of authors, for example references 4 and 5, have postulated that the interaction of temperature fluctuations from the combustor with either the turbine or the nozzle can also produce low frequency noise. Aerodynamic noise from the flow over the various engine struts and surfaces could also be a source of low frequency core noise. The second factor contributing to the difficulty in making core noise predictions is the complexity of the propagation path. For noise originating in the combustor, the noise must propagate through the turbine, tailpipe, nozzle, jet mixing region, and finally to the far-field. This difficulty in making core noise predictions results in a need to determine core noise levels experimentally.

Measurement of core noise is made difficult by the fact that both jet noise and core noise tend to peak in the same frequency range. Both are broadband noise sources and are nearly impossible to distinguish from each other in the far-field spectra. Since the in-flight reduction of jet noise is greater than that of core noise, core noise can be a major noise source from a flying aircraft but will be less evident under static conditions. Thus, it may be important to know the level of the core noise even when jet noise dominates the static noise from an engine.

One method of estimating core noise from static engine data is to subtract from the total measured noise, estimates of all other noise sources. The remainder is assumed to be core noise. This method is applicable only at power settings (usually low power) where the core noise is a significant contributor to the total noise. The method also assumes that the other noise sources can be predicted accurately. Estimates at power settings other than those where core noise dominates are made by extrapolation.

Other techniques for measuring core noise levels have been proposed. Grande (ref. 6) measured the acoustic field within an extension of the core engine tailpipe of a JT8D engine. Assuming no energy loss at the tailpipe nozzle, the far-field core noise power level was determined. Recent tests on the transmission of sound through nozzles (refs. 7 and 8) have shown that the assumption of no energy loss through the nozzle is incorrect. Thus, the radiated sound levels cannot be obtained from internal measurements alone.

Karchmer, et al (ref. 9) used coherence measurements between fluctuating pressures in the combustor of a YF102 turbofan engine and far-field acoustic pressures to estimate the far-field combustor associated noise. Those results were limited to core noise coming from the combustor, and did not include other core noise sources not correlated with the combustor pressure fluctuations.

Parthasarathy, et al. (ref. 10) have proposed a technique for determining core noise using cross-spectra of pairs of far-field microphones. The technique assumes that jet noise is the only contaminating noise source in the far-field, and that

*Aerospace Engineer, Fluid Mechanics and Acoustics Division.

the directivity of the jet noise is known. Further, the method postulates that since the sources of jet noise are in motion relative to the microphones, the Doppler shift between the source and the microphones will cause the jet noise to be incoherent over widely separated directions. The core noise, originating from a stationary source, is assumed to remain coherent for all angular separations.

A new technique is presented in this paper for directly determining core noise levels. To determine the core noise at a particular far-field location, this technique requires that the fluctuating pressure be measured at three locations. Two of the measurement locations are within the engine core and the third is at the far-field position of interest. The cross spectra of these measurements are used to estimate the levels of the far-field noise that propagated from the engine core. No knowledge of the other noise sources contributing to the far-field is required. The technique, referred to as the three-signal coherence technique, was applied to signals measured from an AVCO Lycoming YF102 turbofan engine. Measured fluctuating pressures in the combustor and at the core nozzle exit were used along with far-field noise measurements. Measured core noise levels as a function of frequency and radiation angle are presented for a range of power settings. At low paper settings, where core noise was a significant contributor to the total noise, the measured core noise levels are compared with levels estimated by subtracting predicted jet and fan noise from the total noise. Comparisons are also made with predicted levels and with levels determined using a two-signal coherence technique.

Core Noise Measurement Technique

The present technique provides a method for directly measuring the far-field noise levels originating in the core of an aircraft engine. The technique requires that the fluctuating pressure be measured in the far-field and at two locations in the engine. Because other engine noise sources contribute to the far-field measurement, the far-field measurement cannot be used by itself for determining core noise. However, if a fluctuating pressure is measured within the engine core, the cross-spectrum between the core measurement and the far-field measurement can be calculated. The cross-spectrum between two signals is the product of the spectra of the correlated portions of the two signals. The far-field pressure, P_F, can be written as the sum of a portion that comes from the engine core, P_{F_c}, and a portion from other engine noise sources, P_{Fos},

$$P_F = P_{F_c} + P_{Fos} \tag{1}$$

It is also assumed that the pressure measurement in the engine core is composed of a portion that propagates to the far-field and some non-propagating contamination. The portion that propagates to the far-field will be referred to as "signal." The remainder which does not propagate to the far-field will be referred to as "noise." For an arbitrary location in the engine core, x, this relation is given by:

$$P_x = P_{x_s} + P_{x_n} \tag{2}$$

P_x pressure fluctuation measured in engine core

P_{x_s} portion of P_x that propagates to the far-field

P_{x_n}, portion of P_x that does not propagate to the far-field

This representation of the measurements is shown schematically in figure 1.

If the measurement of the pressure fluctuations in the engine core is made near the core exit, then all of the core noise will contribute to the measurement at that location. The magnitude of the cross-spectrum of the pressure fluctuation at the core exit, P_{exit}, and the far-field pressure, P_F, will then be

$$\left|G_{P_{exit}P_F}(\omega)\right| = \left|P_{exit_s}(\omega)\right| \times \left|P_{F_c}(\omega)\right| \tag{3}$$

The desired quantity is the spectrum of the far-field signal that comes from the engine core, $|P_{F_c}(\omega)|^2$. If all of the pressure fluctuations in the engine core resulted in a signal propagating to the far-field then there would be no "noise" in this measurement, i.e., $P_{exit} = P_{exit_s}$ for $P_{exit_n} = 0$. Then for $P_{exit_n} = 0$

$$\left|{}_2P_{F_c}(\omega)\right|^2 = \frac{\left|G_{P_{exit}P_F}(\omega)\right|^2}{\left|P_{exit}(\omega)\right|^2} \tag{4}$$

The subscript 2, preceding the symbol P_{F_c} in equation (4), is used to indicate that only two signals, one in the far-field and one at the core exit, are used to compute this estimate of the far-field core noise. The estimate of the far-field core noise, $|{}_2P_{F_c}(\omega)|$, using equation (4) would usually be referred to as the "coherent output power spectrum" (ref. 11). In this paper, however, $|{}_2P_{F_c}(\omega)|$, will be called "the two signal coherent output power spectrum." For the case where there is contamination of the measure core pressure fluctuations, i.e., $P_{exit_n} \neq 0$, the computed "two signal coherent output power spectrum" will give a low estimate of the far-field core noise. In order to overcome this problem, a measurement at another location in the engine core is used. This second engine core measurement is used, along with the measurements at the core exit and in the far-field, to determine the transfer function between the core exit and the far-field. Consider a measurement made in the combustor, P_c. Again it will be assumed that this measurement consists of a signal and noise. From equation (2), with the subscript x replaced by c to indicate a measurement made in the combustor

$$P_c = P_{c_s} + P_{c_n} \tag{5}$$

By definition, the "noise" in the combustor, P_c, does not correlate with the far-field measurement. However, it is possible that the noise in the combustor, P_{c_n}, will correlate with the noise at the core exit, P_{exit_n}. If it can be assumed that the noise in the combustor does not correlate with the noise at the core exit, then the transfer function, h, from the core exit to the far-field is given by the ratio of the cross-spectrum between the combustor pressure and the far-field measure-

ment to the cross-spectrum between the combustor pressure and the core exit pressure.

$$h = \frac{P_{F_c}(\omega)}{P_{exit}(\omega)} = \frac{G_{P_c P_F}(\omega)}{G_{P_c P_{exit}}(\omega)} \qquad (6)$$

One possible source of "noise" in the engine measurements is pseudosound. Pseudosound, also referred to as hydrodynamic noise, is a locally correlating pressure fluctuation which is convected with the fluid flow. The correlation between the pseudosound at two locations will decrease as the distance between the locations increases. Thus by maximizing the separation of the two engine probes, the correlation between the pseudosound at the probes will be minimized.

Another possible source of "noise" in the engine measurements is higher order acoustic modes present in the engine but not propagating to the far-field. For example, using the relations in reference 12, the hard wall cut-on frequency of the first circumferential mode is calculated to be about 380 Hz in the combustor of the YF102 engine, but is calculated to be cut off up to 730 Hz at the YF102 core exit. Below 730 Hz,, this mode is not expected to radiate very efficiently to the far-field. However, the mode will exist in the combustor, where it is cut-on, and downstream of the combustor even where it is cut-off. At locations where the mode is cut-off, the magnitude of the mode will decay exponentially with axial distance. Consider a first order circumferential mode at 400 Hz. Using the cut-on frequency at the turbine exit, 480 Hz, as an estimate of the average cut-on frequency for the distance between the combustor and the core exit, the decay rate at 400 Hz is calculated to be 23 dB/m. The toal distance from the combustor to the core exit for the YF102 engine is about 0.8 m. Thus at 400 Hz, the level of the first circumferential mode at the core exit will be 18 dB less than the level in the combustor. Thus, if in the combustor at 400 Hz the first circumferential mode is higher than the plane wave mode by about 9 dB, the cross spectrum between the fluctuating pressure in the combustor and that at the core exit would be about 3 dB higher than that for the plane wave only. This 3 dB increase in the cross-spectrum between the engine probes would result in a 3 dB underprediction of the far-field core noise. The error would be reduced if some of the first order mode did in fact radiate to the far-field. To determine the actual modal content, a number of probes would be required at each engine location of interest.

For the method presented in this report, it will be assumed that the error due to higher order modes is negligible. It will also be assumed that the engine probes are sufficiently separated so that no correlation exists between any other "noise" at one engine probe location and that at the other. With these assumptions, the spectrum of the far-field signal that comes from the engine core is then given by

$$\left|{}^{3}P_{F_c}(\omega)\right|^2 = \frac{\left|G_{P_{exit}P_F}(\omega)\right| \times \left|G_{P_c P_F}(\omega)\right|}{\left|G_{P_c P_{exit}}(\omega)\right|} \qquad (7)$$

where the notation $|{}^{3}P_{F_c}(\omega)|^2$ is used to indicate core noise levels as determined using the three signal coherence techniques.

Application of the Three Signal Coherence Technique

The technique presented herein for determining far-field core noise levels from gas turbine aircraft engines was applied to tape recorded signals, previously obtained during the tests reported in references 13, 14, and 15. These tests were conducted on an AVCO Lycoming YF102 turbofan engine. A short description of this engine and these tests is presented in the next section. This is followed by a section describing the data analysis procedure used to evaluate equation (7) in the preceding section.

Engine and Test Description

The YF102 is a turbofan engine with a rated thrust of 33 kN and a bypass ratio of 0. The engine core consists of an eight-stage compressor, a reverse flow annular combustor and a four-stage turbine. A cutway illustration of the engine is shown in figure 2. Acoustic testing of the engine was conducted at an outdoor test stand with the engine centerline 2.9 m above a hard surface ground plane. A photograph of the engine on the test stand is shown in figure 3. The engine was configured with a bellmouth inlet and separate core and fan exhaust nozzles. Additional details on the engine and its performance are given in reference 16.

During the tests, simultaneous measurements of pressure fluctuations within the engine and in the far-field were made at eight fan speeds between 30 and 95 percent of maximum speed. Pressure fluctuations were measured at seven different locations in the engine using semi-infinite tube pressure probes. The locations of these measurements are as follows: two just downstream of the compressor exit, about 2 cm apart; one at the combustor entrance; two within the combustor at the same axial location but separated 90° circumferentially; and two within the core tailpipe, one just downstream of the turbine exit and one close to the tailpipe exit plane. A schematic showing the probe locations is shown in figure 4. A detailed description of these probes is presented in reference 15.

Far-field noise measurements were made using an array of sixteen ground-level microphones on a 30.5 m radius circle centered on the exhaust plane of the core nozzle. The microphones were placed on a concrete surface 10° apart from 10° to 160° from the engine inlet axis. The signals from the internal probes and the far-field microphones were FM recorded on magnetic tape in two minute record lengths for later processing.

Data Analysis

The data obtained during the tests were analyzed using a two-channel fast Fourier transform digital signal processor. The processor was capable of direct computation of up to 4096 ensemble averages of 1024 forward or inverse Fourier transforms to yield either time domain (correlation) or frequency domain (cross-spectra, transfer function, or coherence) information. The processor had

built-in 120 dB/octave anti-aliasing filters and provisions for pre-computation delay. The pre-computation delay provision allows one signal to be delayed relative to the other to remove the physical delay due to acoustic transmission. This process minimizes the time delay bias error that would result if the physical time delay were not removed (see ref. 15).

For the technique described in this report, the required quantities to be calculated are: the cross-spectra between the tailpipe exit probe and the far-field; the cross-spectra between an upstream probe (usually one of the combustor probes) and the far-field, and the cross-spectra between the upstream probe and the tailpipe exit probe. The signals were analyzed over a frequency range from 0 to 2400 Hz with a bandwidth of 6 Hz. The cross-spectra between the engine probes and the far-field signals were computed with a pre-computation time delay of 0.083 sec. This pre-computation delay is approximately equal to the acoustic propagation delay of 0.087 sec. The cross-spectra between the engine probes and the far-field were usually computed based on 256 ensemble averages. For the cross-spectra between engine probes, 512 ensemble averages were usually taken and no pre-computation delay was used. Auto-spectra of the signals were computed simultaneously with the cross-spectra. The resultant auto- and cross-spectra were transmitted to an IBM 370 digital computer for the computation of the far-field core noise levels. One-third-octave levels were computed by summing the 6 Hz band levels over the one-third-octave frequency bands. For bands straddling two one-third-octave bands, the level was apportioned between the two one-third-octave bands, assuming white noise in the constant-bandwidth band. All data presented in this paper are for as-measured conditions. No corrections have been made for atmospheric attenuation or ground reflections.

Results and Discussion

The three signal coherence technique presented herein was used to determine core noise levels for the YF102 turbofan engine. These levels were determined as a function of frequency and radiation angle over a range of power settings. Some typical one-third octave spectra and a few narrow band spectra are presented in this section. Also presented is an examination of the sensitivity of these spectra to the location of the upstream engine probe. Next the core noise levels are compared with the total noise and jet noise levels to determine the relative importance of the core noise from this engine. Finally, comparisons are made of core noise levels determined using the three signal coherence technique with predicted core noise levels and with core noise levels determined from the experimental data using other procedures.

Spectra

One-third octave spectra. - Typical far-field, one-third octave core noise spectra obtained using the three signal coherence technique are shown in figure 5 for several power settings. These spectra are for a radiation angle of 120° from the engine inlet. A radiation angle of 120° was chosen because core noise tends to peak at about 120°. The spectra exhibit several peaks. The peak at 125 to 160 Hz, that is clearly evident at the two lower engine speeds, has been identified as being highly coherent with the pressure fluctuations in the combustor (ref. 9). The higher frequency peaks may be associated with the cut-on of higher order modes within the core.

Narrow band spectra. - Narrow band (6 Hz) spectra of far-field core noise determined using the three signal coherence technique and measured far-field total noise are presented in figure 6. The data in figure 6a are for an engine speed of 43 percent and that in figure 6(b) is for an engine speed of 95 percent. As can be seen, the core noise levels are very irregular. This is a direct result of the irregularity in the individual cross-spectra used to compute the measured core noise levels. From equation (7), the cross-spectra used to compute the core noise levels are the cross-spectrum between the core exit and the far-field, the cross-spectrum between the combustor and the far-field, and the cross-spectrum between the combustor and the core exit. These cross-spectra are shown in figures 7(a) to (f) for engine speed of 43 and 95 percent. The irregularity in the cross-spectra is due to the low coherence between measurements. Typical coherences between pairs of measurements at 43 percent speed are shown in figure 8. As can be seen in figure 8, above 200 Hz, the coherences between the combustor probe and either the downstream tailpipe or the far-field are very small. These small coherences result in the large variances in the measured cross-spectra (ref. 9).

Effect of upstream probe location. - The effect of the location of the upstream engine probe on the core noise levels determined using the three signal coherence techniques is presented in figure 9. Three different upstream probe locations were used for this comparison, two in the combustor and one at the tailpipe inlet. The combustor probe (circle symbols) that was used for the other figures in this report, is in-line with the tailpipe probes. The second combustor probe (triangular symbols) is at the same axial location but is separated circumferentially by 90°. In all cases, the tailpipe exit probe was used as the downstream probe. The core noise levels measured using each of the upstream probes are compared in figure 9 for several engine speeds. As can be seen, the measured core noise levels are not sensitive to the location of the upstream probe with the largest variance occurring at 95 percent speed.

Noise Component Comparisons

In figure 10, the measured core noise levels are compared with measured far-field total noise levels at 120° from the engine inlet for several engine speeds. Also shown in figure 10 are jet and fan noise levels predicted using the methods of references 17 and 18, respectively. At the lowest engine speed of 30 percent, (fig. 10(a)), the core noise is dominant over nearly the entire frequency range and accounts for nearly all of the far-field noise shown. An anomaly occurs at 315 Hz where the measured core noise exceeds the total by several dB. At this speed, the jet noise contributes only at frequencies below 100 Hz and fan noise contributes above 630 Hz. As the engine speed is increased from 30 percent to 50 percent (figs. 10(b) to (d), the contribution of jet noise increases at low frequencies; however, core noise continues to dominate in the frequency range from 100 to

800 Hz. At 60 percent engine speed, figure 10(e), the jet and core noise levels are about equal. At the highest speeds, figures 10(f) and (g), the jet noise dominates.

The relative contribution of jet and core noise can also be seen by comparing overall sound pressure levels. In figure 11, total, core and jet overall sound pressure levels from 50 to 1000 Hz are plotted against engine speed. Again the total and core levels are measured and the jet levels are predicted. Again the dominance of core noise at low speeds and jet noise at high speeds is evident. However, the comparison in figure 11 is for static conditions. At typical flight conditions, the jet noise levels would be decreased about 6.5 dB relative to the core noise at 95 percent engine speed. This would make the jet and core noise levels nearly equal even at takeoff power settings. This example illustrates the importance of knowing the core noise levels even when, at static conditions, the jet noise may dominate.

Comparisons With Other Core Noise Estimates

At low power settings, where the core noise dominates the far-field levels, an estimate of core noise levels can be obtained by subtracting the predicted jet and fan noise from the total noise. At the higher power settings where the jet noise is nearly equal to the total, small errors in either the measured total noise or the predicted jet noise would result in large errors in core noise. Comparisons of core noise levels obtained by subtracting predicted values of jet and fan noise from the total noise with levels obtained using the three-signal coherence method are shown in figure 12 for several angles at 30 percent engine speed and at 120° for 37 percent and 43 percent engine speed. Excellent agreement was obtained for frequencies up to 400 Hz. Above 400 Hz, the three-signal coherence technique gives levels that are 2 to 5 dB below those obtained by subtracting jet and fan noise from the total noise. Several reasons for this difference can be postulated: (1) Fan noise levels were underpredicted; (2) Coherence existed between the non-radiating noise at the two engine probes; and (3) The low levels of coherence between the signals resulted in a bias in the core noise levels. The fan noise levels were predicted using the method of reference 18. This method has an exponential decrease in the fan noise levels as the frequency decreases. In reference 19, a fan noise prediction method is given which uses a linear decrease in level with decreasing frequency. This linear relation would give higher levels of predicted fan noise and hence lower levels of core noise. A comparison of the fan noise levels using the two prediction shapes is shown in figure 13. The impact of using the reference 19 fan noise prediction on core noise obtained by subtracting predicted jet and fan noise from the total noise is shown in figure 14. Here new estimates of core noise using reference 19 fan noise levels are compared with core noise levels obtained using the three-signal coherence technique. Better agreement between the two estimates is obtained at higher frequencies. However, the better agreement using the fan noise prediction of reference 19 shoud not be used to judge which fan noise prediction procedure is better. This exercise only illustrates the sensitivity of a commonly used core noise determination technique to the knowledge of other engine noise sources.

As mentioned in the description of the core noise measurement technique, in the absence of non-radiating noise at the tailpipe exit, the far-field core noise could be calculated using a single engine probe. In figure 15, the core noise levels determined using the three-signal coherence technique are compared with those determined using only the tailpipe exit probe. The spectrum determined using only the tailpipe exit probe was referred to as the "two-signal coherent output power spectrum" and is evaluated using equation (4). In the presence of non-radiating noise at the tailpipe exit, the "two-signal coherent output power spectrum" will give a low estimate of the far-field core noise. It can be seen in figure 15 that this is indeed the case. Except for a few isolated frequencies, the "two-signal coherent output power spectrum" is consistently several dB below the core noise levels as determined by the three-signal coherence technique.

Core noise levels determined using the three-signal coherence technique were also compared with predicted levels using the core noise prediction methods of references 2 and 3. A comparison of the spectra at an angle of 120° and 30 percent engine speed is shown in figure 16. The method of reference 2 predicts the core noise at low frequencies but overpredicts at high frequencies by several dB. The method of reference 3 underpredicts the levels at low frequencies and overpredicts at high frequencies by 5 to 7 dB. At 95 percent speed, figure 16, both methods overpredict the data. A comparison of overall sound pressure level directivities is shown in figure 17 for 30 percent speed. The predicted directivities bracket the data and agree with the data to within ±2 dB. In general, the predicted levels are in fair agreement with the data.

Summary of Results

A technique for directly measuring core noise levels from aircraft engines was presented. The technique makes it possible to measure core noise levels even when other noise sources dominate. By measuring the fluctuating pressures in the far-field and at two locations within the engine, the effects of contamination of the measurements within the engine by non-radiating noise are eliminated. The technique was used to measure core noise levels from an AVCO Lycoming YF102 turbofan engine. Excellent agreement between levels measured using this technique and those obtained by subtracting predicted jet and fan noise from the measured total noise was obtained for frequencies below 500 Hz. Above 500 Hz the agreement is dependent on the fan noise prediction used. Good agreement was obtained using a fan noise prediction procedure have a linear decrease in fan noise with decreasing frequency. A comparison of predicted core noise levels with the measured levels showed fair agreement between predicted and measured levels for the YF102 engine.

REFERENCES

1. Heldenbrand, R. W. and Norgren, W. M., "AiResearch QCGAT Program," AiResearch Mfg. Co., Phoenix, AZ, AIRESEARCH-21-3071, Jan. 1979. (NASA CR-159758).

2. Huff, R. G., Clark, B. J., and Dorsch, R. G., "Interim Prediction Method for Low Frequency Core Engine Noise," TM X-71627, 1974.

3. Matta, R. K., Sandusky, G. T., and Doyle, V. L., "G.E. Core Engine Noise Investigation - Low Emission Engines," General Electric Co., Cincinnati, OH, Feb. 1977. (FAA-RD-77-4, AD-A048590).

4. Strahle, W. C., Muthukrishan, M., and Neale, D. H., "Experimental and Analytical Separation of Hydrodynamic, Entropy and Combustion Noise in a Gas Turbine Combustor," AIAA Paper 77-1275, Oct. 1977.

5. Pickett, G. F., "Core Engine Noise Due to Temperature Fluctuation Convecting Through Turbine Blade Rows," AIAA Paper 75-528, Mar. 1975.

6. Grande, E., "Exhaust Noise Field Generated in the JT8D Core Engine - Noise Floor Presented by the Internal Noise Sources," J. Acoust. Soc. Am., Vol. 55, Jan. 1974, pp. 30-34.

7. Ahuja, K. K., Salikuddin, M., Burrin, R. H., and Plumblee, H. E., Jr., "A Study of the Acoustic Transmission Characteristics of Suppressor Nozzles," Lockheed-Georgia Co., Marietta, CA, June 1980. (NASA CR-165133).

8. Bechert, D., Michel, U., and Pfizenmaier, E., "Experiments on the Transmission of Sound Through Jets," AIAA Paper 77-1278, Oct. 1977.

9. Karchmer, A. M., Reshotko, M., and Montegani, F. J., "Measurement of Far-Field Combustion Noise from a Turbofan Engine Using Coherence Functions," NASA TM-73748, 1977.

10. Parthasarathy, S. P., Cuffel, R. F., and Massier, P. F., "Separation of Core Noise and Jet Noise," AIAA Paper 79-0589, Mar. 1979.

11. Halvorsen, W. G., and Bendat, J. S., "Noise Source Identification Using Coherent Output Power Spectra," Sound and Vibration, Vol. 9, Aug. 1975, pp. 15, 18-24.

12. Morse, P. M. and Ingard, K. U., Theoretical Acoustics, McGraw-Hill, New York, 1968, pp. 492-514.

13. Karchmer, A. and Reshotko, M., "Core Noise Source Diagnostics on a Turbofan Engine Using Correlation and Coherence Techniques," NASA TM X-73535, 1976.

14. Reshotko, M., Karchmer, A., Penko, P., and McArdle, J., "Core Noise Measurements on a YF-102 Turbofan Engine," NASA TM X-73587, 1977.

15. Karchmer, A. M., "Identification and Measurement of Combustion Noise from a Turbofan Engine Using Correlation and Coherence Techniques," NASA TM-73747, 1977.

16. McArdle, J. G., Homyak, L., and Moore, A. S., "Static Test-Stand Performance of the YF-102 Turbofan Engine with Several Exhaust Configurations for the Quiet Short-Haul Research Aircraft (QSRA)," NASA TP-1556, 1979.

17. Stone, J., "Interim Prediction Method for Jet Noise," NASA TM X-71618, 1974.

18. Heidmann, M., "Interim Prediction Method for Fan and Compressor Source Noise," NASA TM X-71763, 1975.

19. Dunn, D. G., and Peart, N. A., "Aircraft Noise Source and Contour Estimation," Boeing Commerical Airplane Co., Seattle, WA, D6-60233, July 1973. (NASA CR-114649).

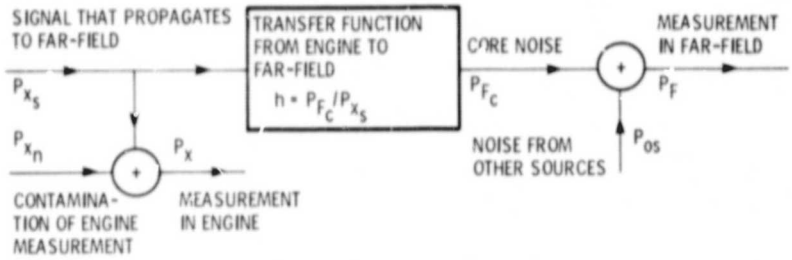

Figure 1. - Schematic representation of measured pressure fluctuations in the engine core and far-field.

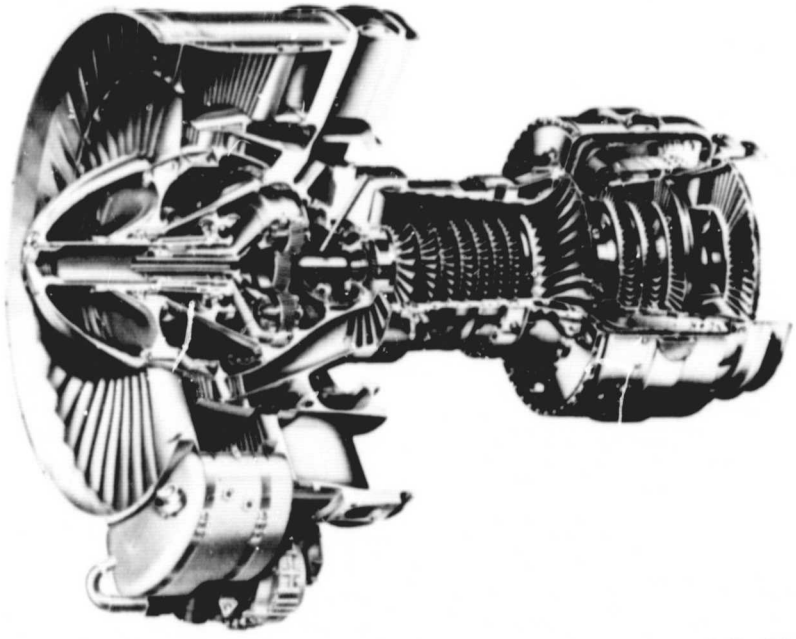

C-76-781

Figure 2. - Cutaway illustration of YF102 turbofan engine.

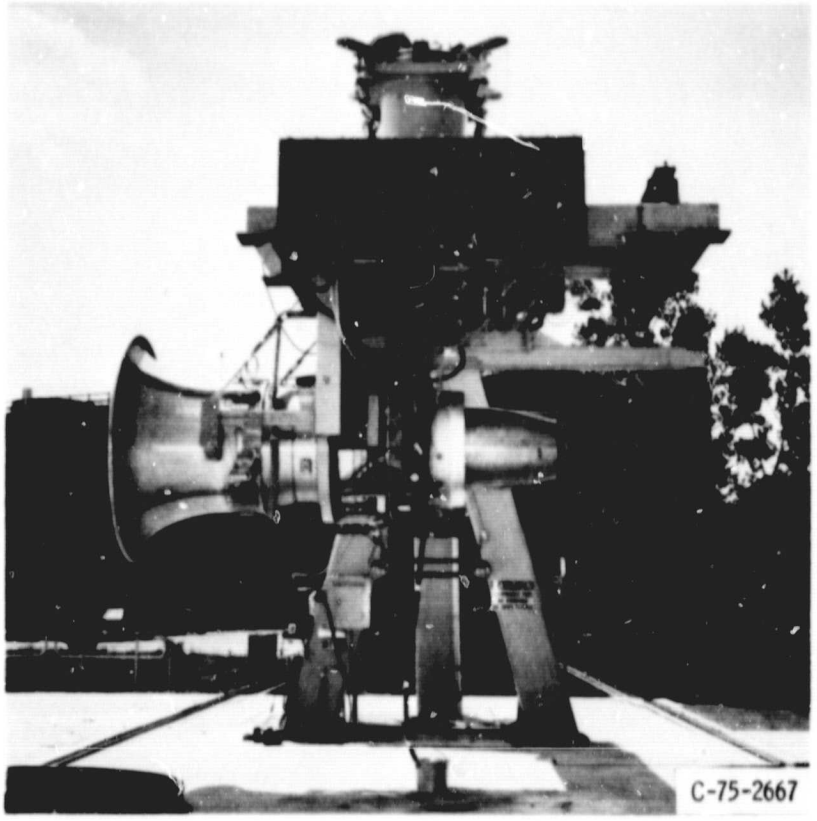

Figure 3. - YF102 turbofan engine on test stand.

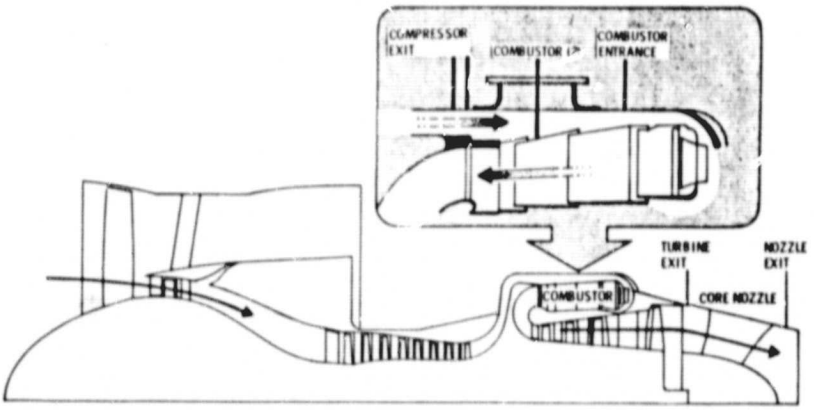

Figure 4. - Schematic showing core probe locations.

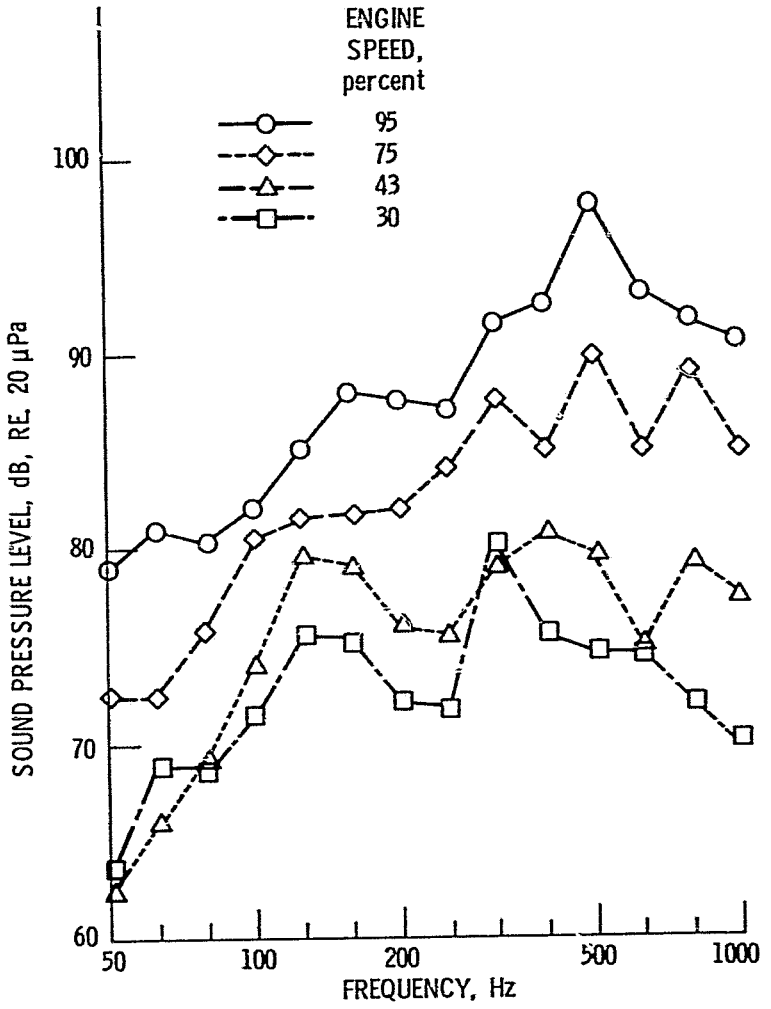

Figure 5. – Measured core noise spectra for several engine speeds at 120° from the engine inlet.

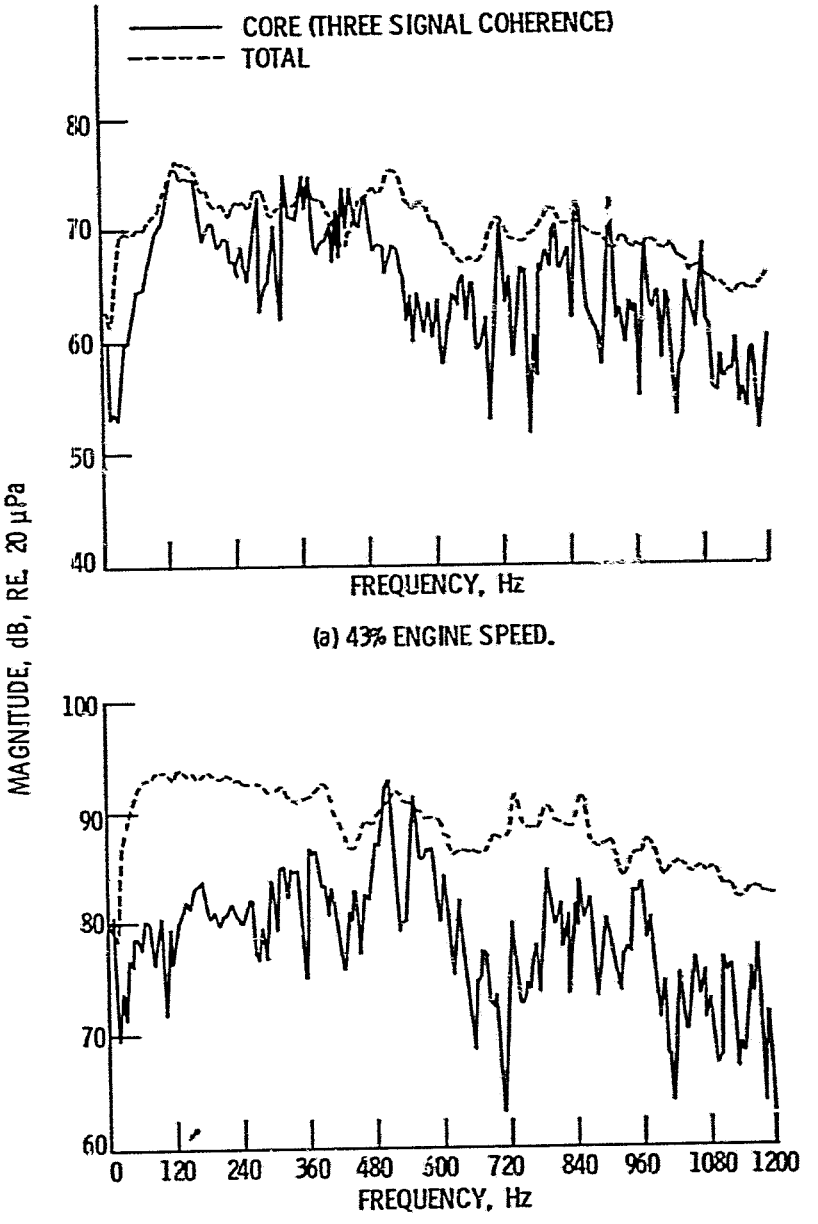

(a) 43% ENGINE SPEED.

(b) 95% ENGINE SPEED.

Figure 6. – Comparison of far-field core and total noise narrow band (6 Hz) measured spectra at 120° from engine inlet.

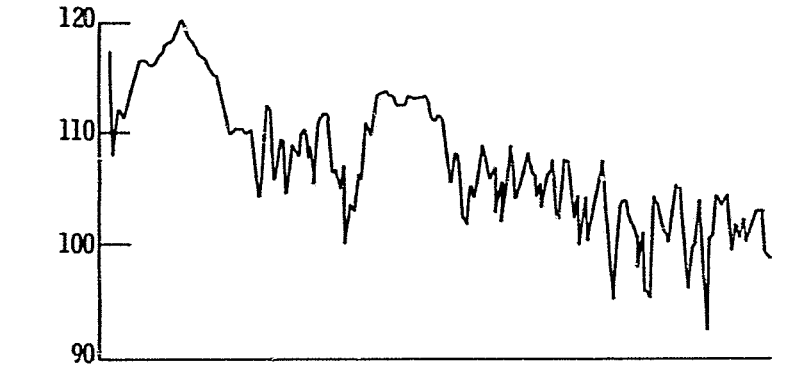

(a) COMBUSTOR TO TAILPIPE EXIT, 43% SPEED.

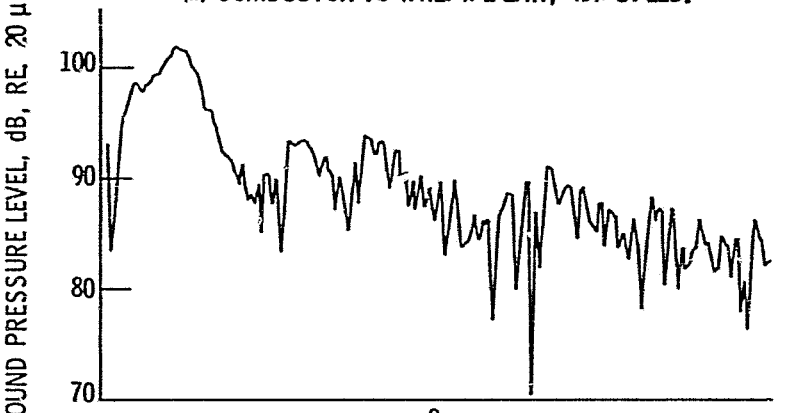

(b) COMBUSTOR TO 120° FAR-FIELD, 43% SPEED.

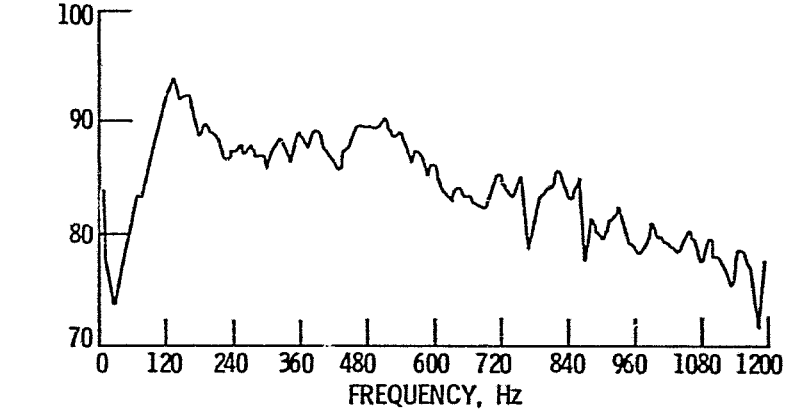

(c) TAILPIPE EXIT TO 120° FAR-FIELD, 43% SPEED.

Figure 7. - Measured cross-spectra.

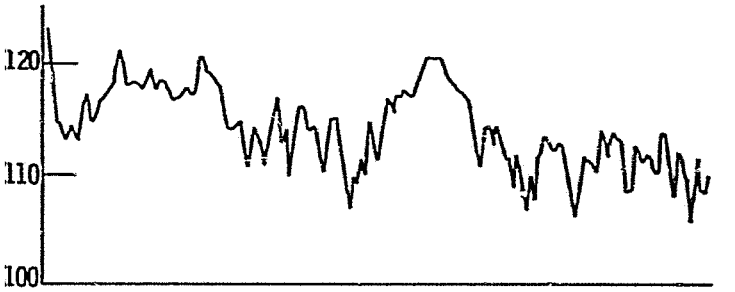

(d) COMBUSTOR TO TAILPIPE EXIT, 95% SPEED.

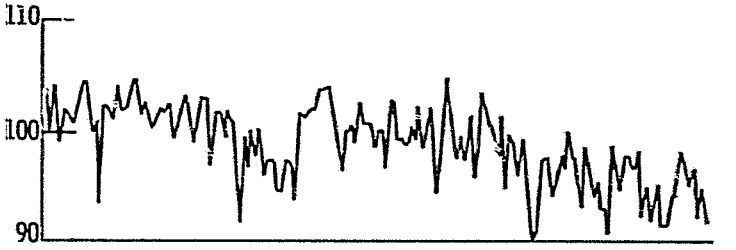

(e) COMBUSTOR TO 120° FAR-FIELD, 95% SPEED.

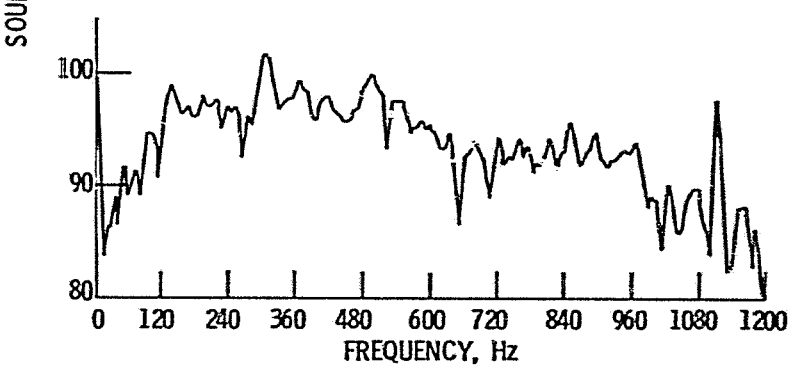

(f) TAILPIPE EXIT TO 120° FAR-FIELD, 95% SPEED.

Figure 7. - Concluded.

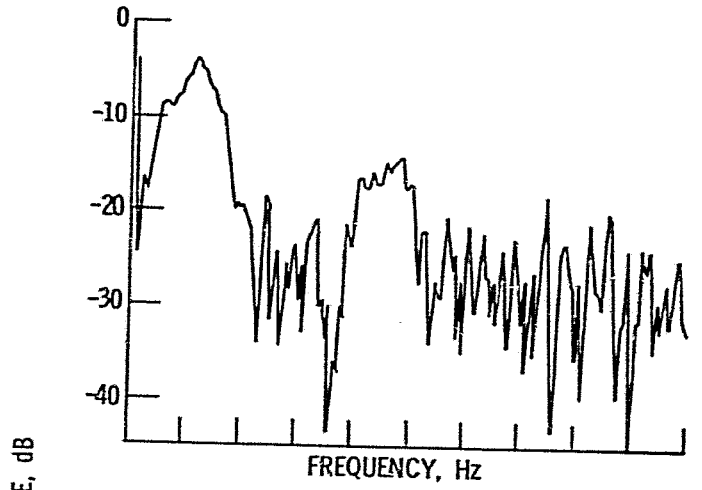

(a) COHERENCE BETWEEN COMBUSTOR AND TAILPIPE EXIT PRESSURES, 43% SPEED.

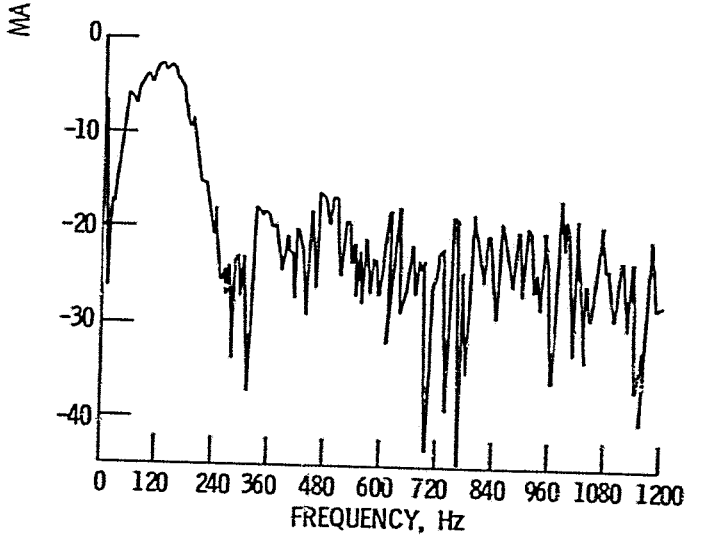

(b) COHERENCE BETWEEN COMBUSTOR AND 120° FAR-FIELD PRESSURE, 43% SPEED.

Figure 8. - Measured coherences.

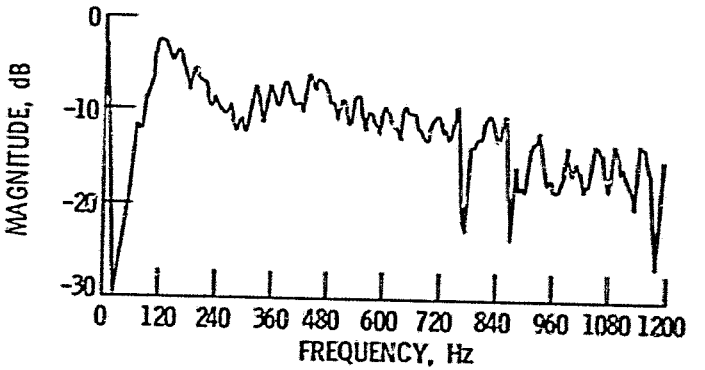

(c) COHERENCE BETWEEN TAILPIPE EXIT AND 120° FAR-FIELD PRESSURE, 43% SPEED.

Figure 8. - Concluded.

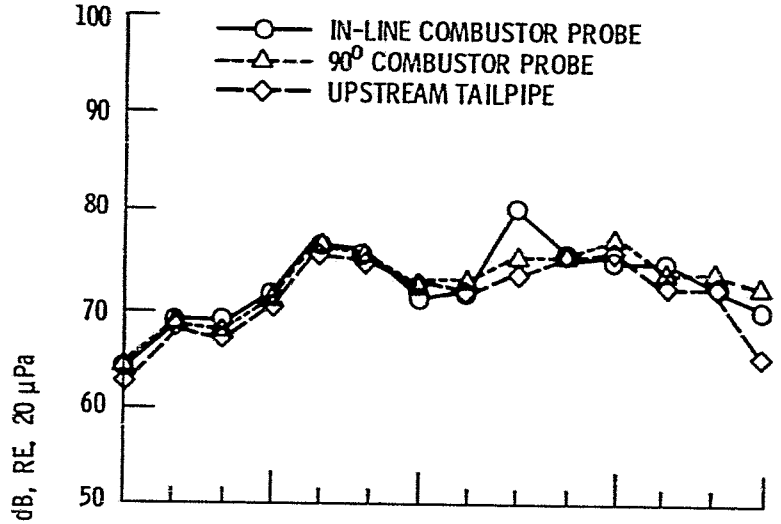

(a) 30% ENGINE SPEED.

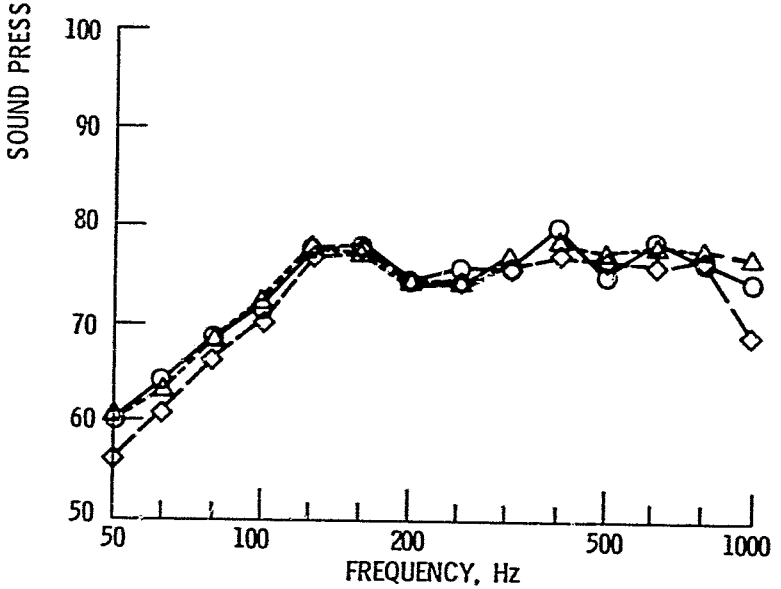

(b) 37% ENGINE SPEED.

Figure 9. - Comparison of measured core noise levels at 120° from engine inlet for several upstream probe locations.

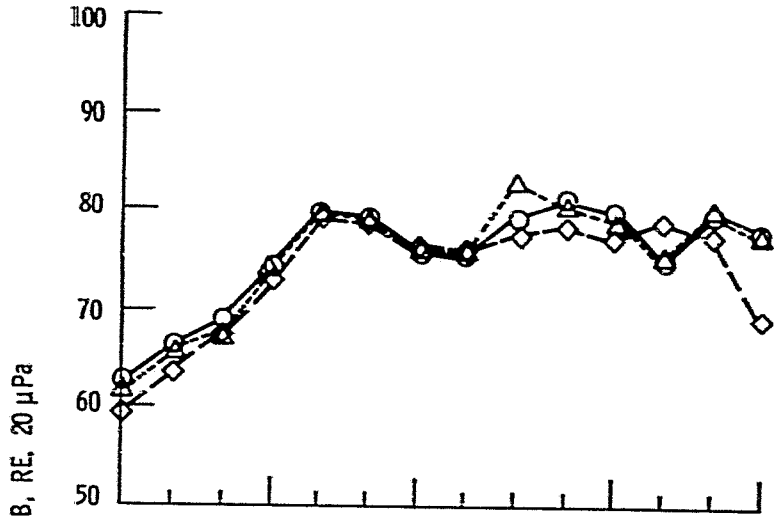

(c) 43% ENGINE SPEED.

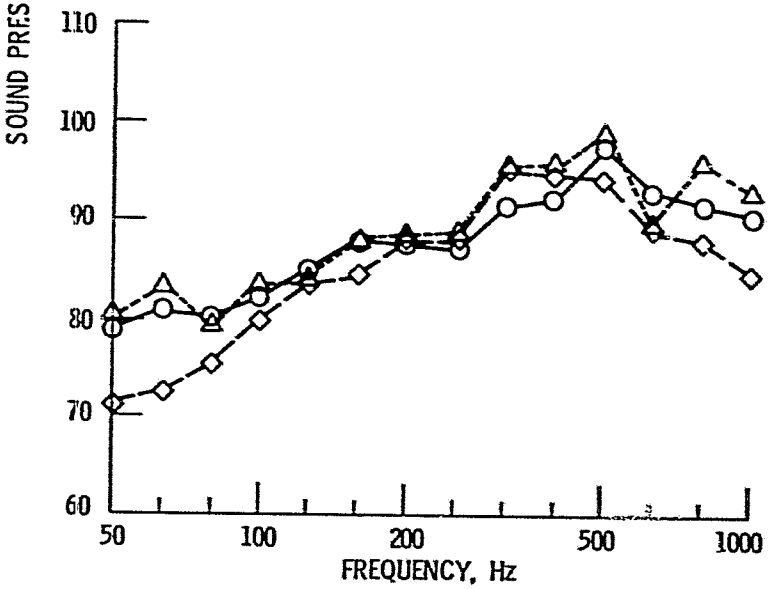

(d) 95% ENGINE SPEED.

Figure 9. - Concluded.

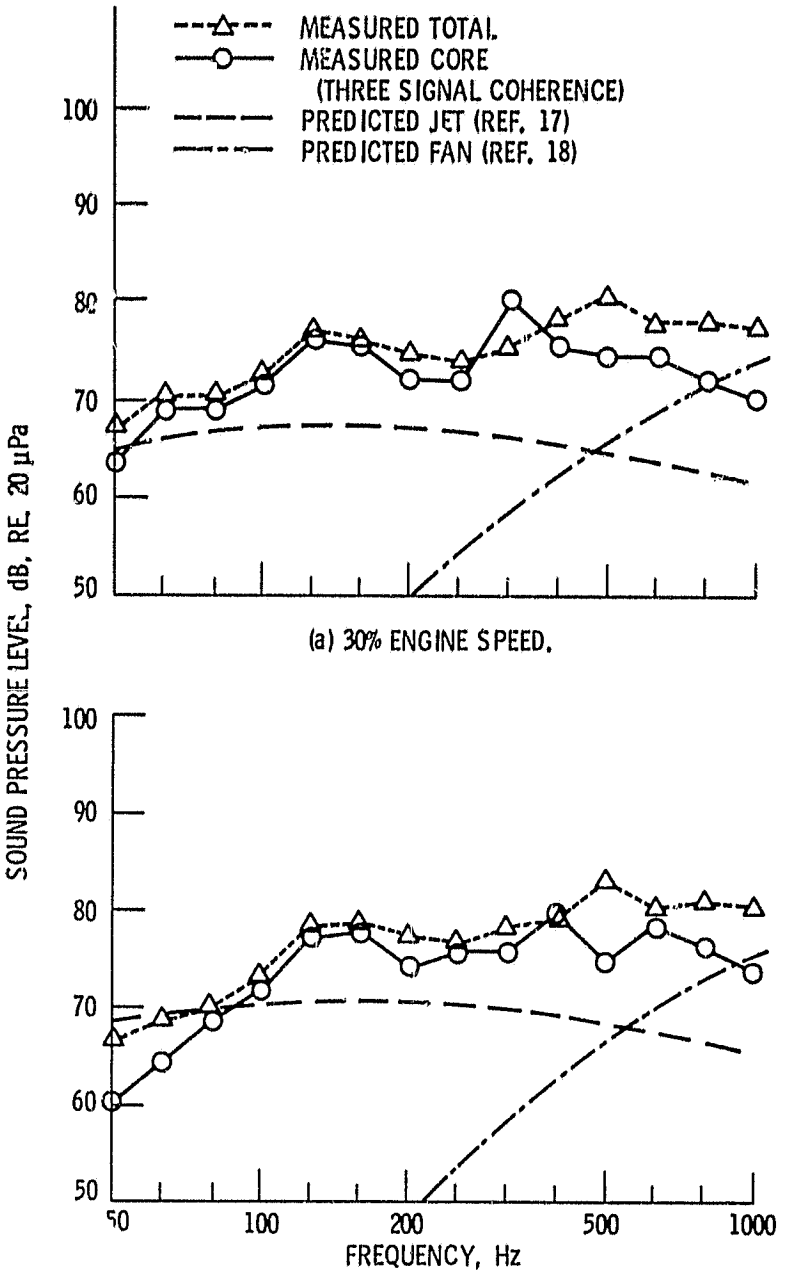

(a) 30% ENGINE SPEED.

(b) 37% ENGINE SPEED.

Figure 10. - Comparison of core, jet, and fan noise levels to total noise at 120^0 from the engine inlet.

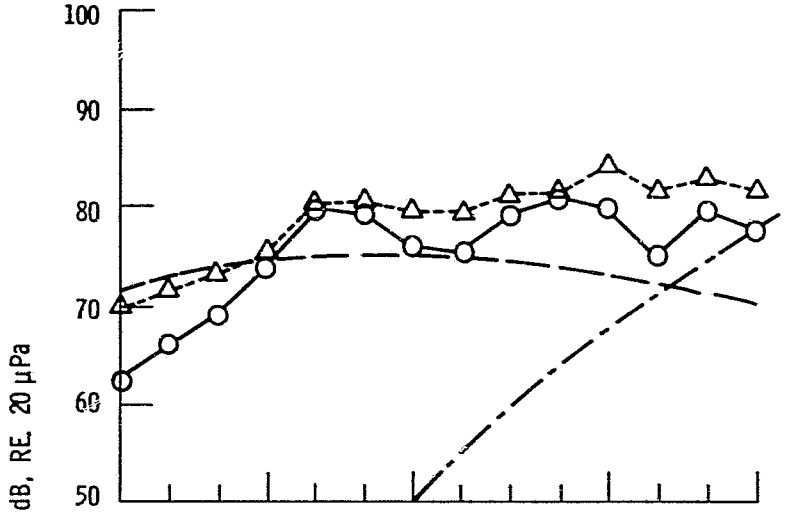

(c) 43% ENGINE SPEED.

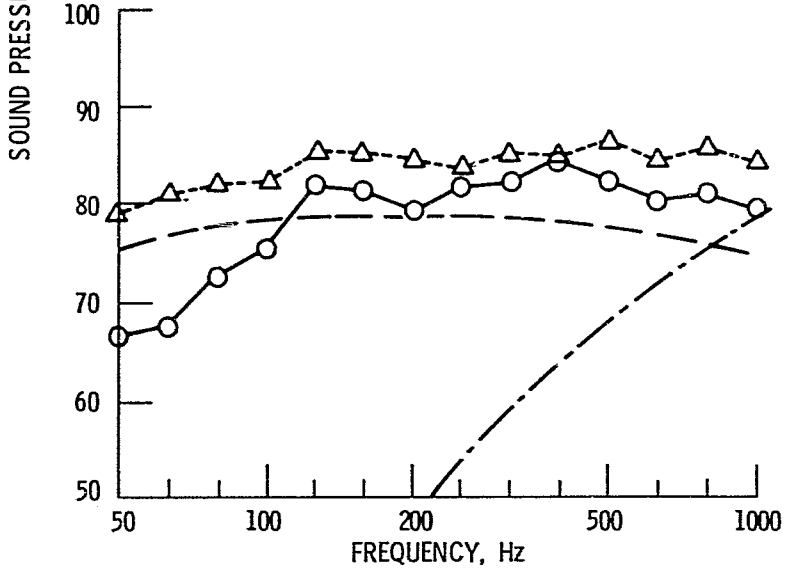

(d) 50% ENGINE SPEED.

Figure 10. - Continued.

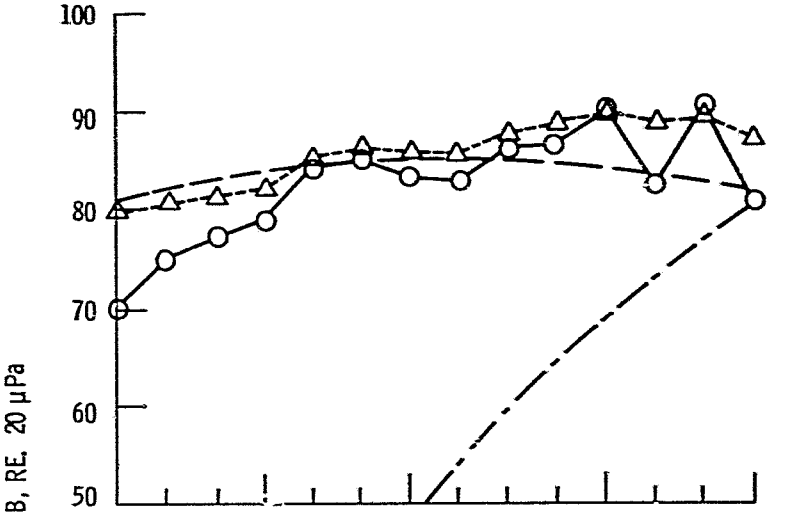

(e) 60% ENGINE SPEED.

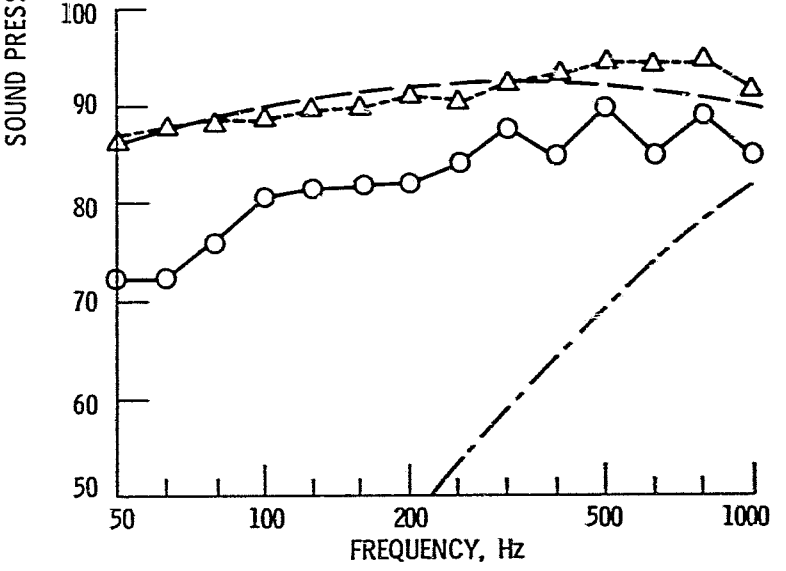

(f) 75% ENGINE SPEED.

Figure 10. - Continued.

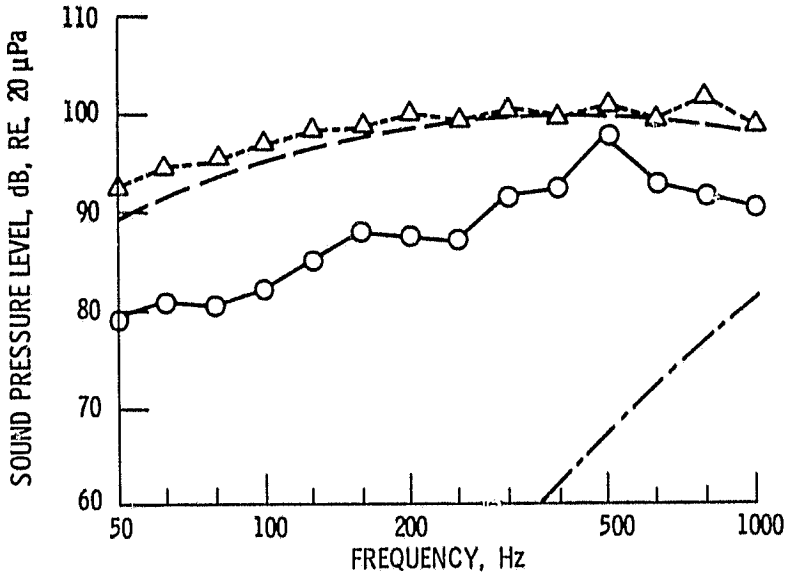

(g) 95% ENGINE SPEED.

Figure 10. - Concluded.

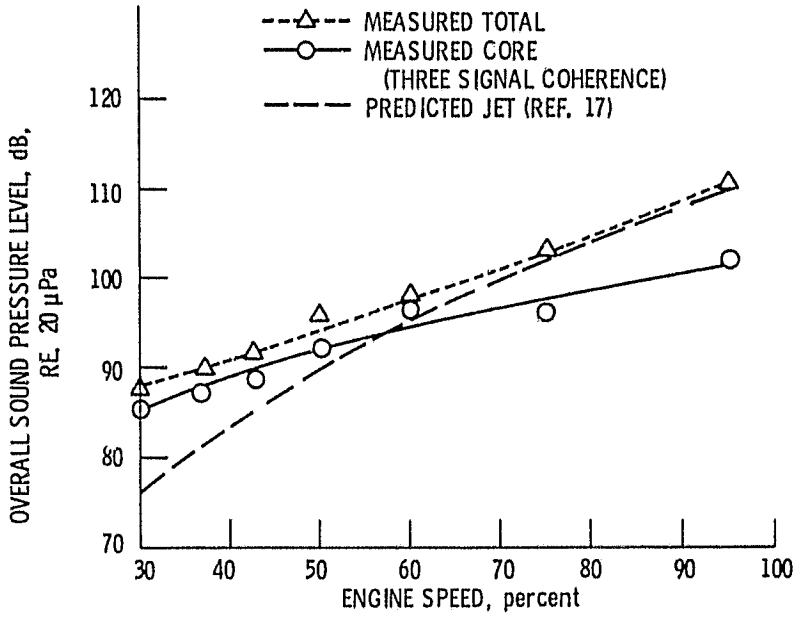

Figure 11. - Variation of measured total and core and predicted jet noise overall sound pressure levels with engine speed at 120^{0} from engine inlet, (frequency range 50-1000 Hz).

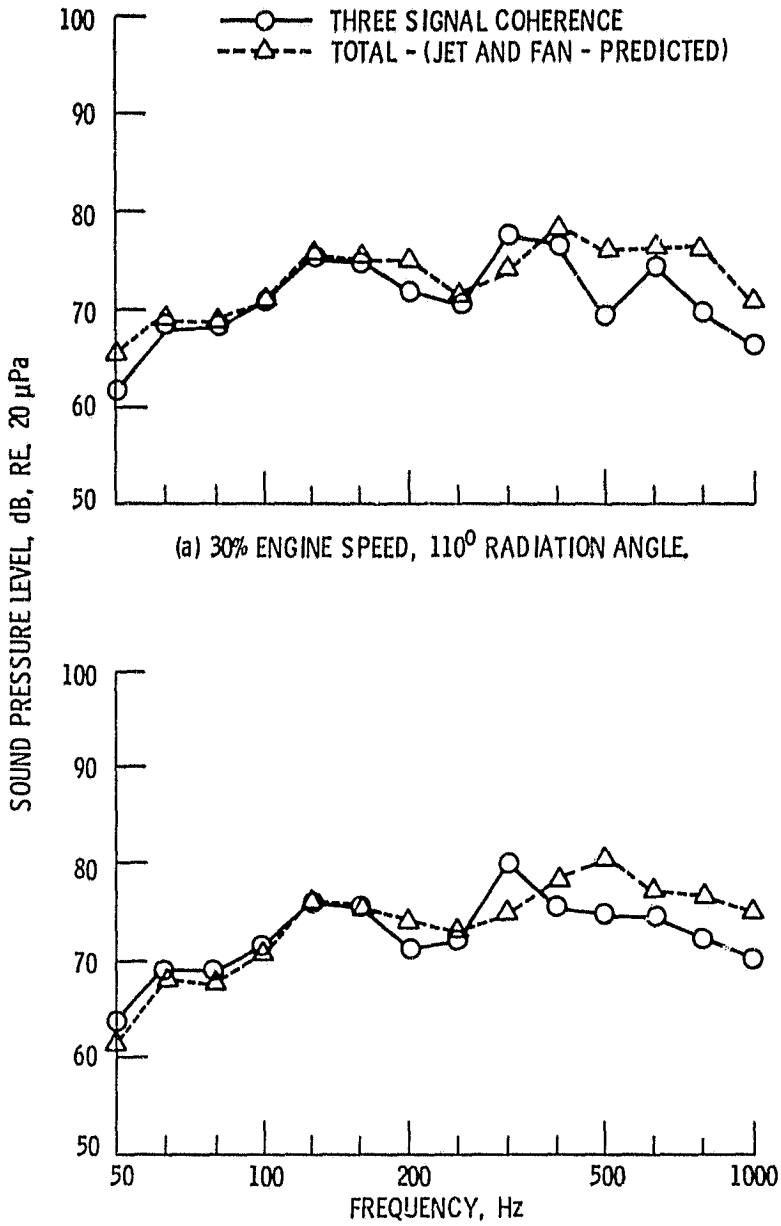

(a) 30% ENGINE SPEED, 110° RADIATION ANGLE.

(b) 30% ENGINE SPEED, 120° RADIATION ANGLE.

Figure 12. - Comparison of core noise measured using the three signal coherence technique with core noise estimated by subtracting predicted jet (ref. 17) and fan (ref. 18) from total noise.

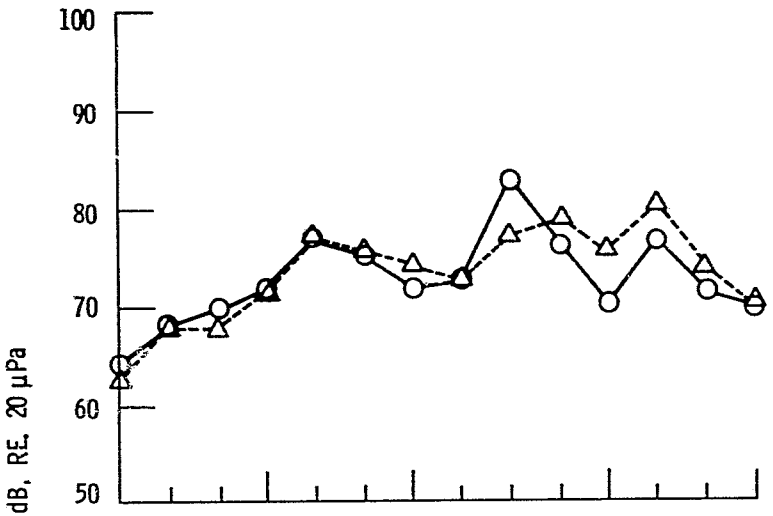

(c) 30% ENGINE SPEED, 130° RADIATION ANGLE.

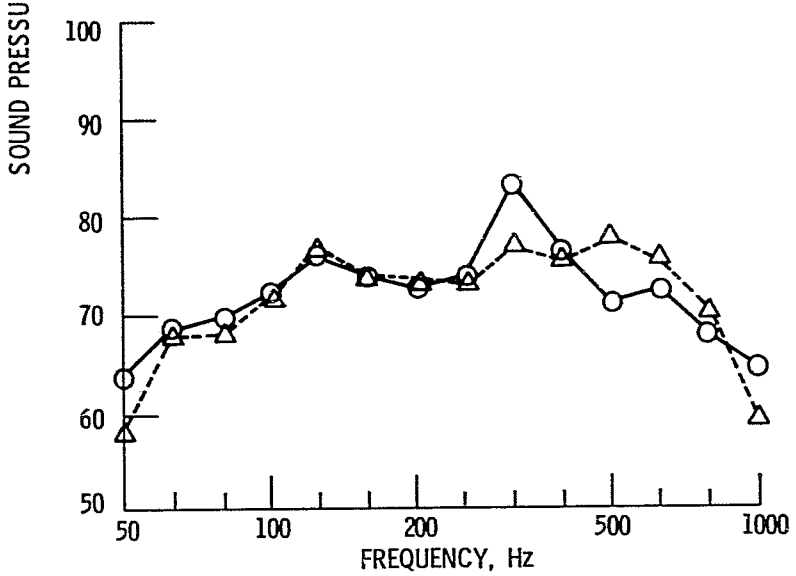

(d) 30% ENGINE SPEED, 140° RADIATION ANGLE.

Figure 12. - Continued.

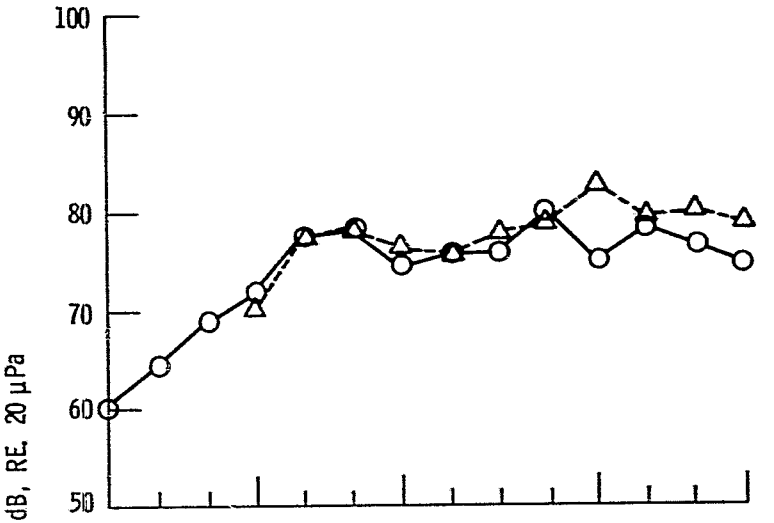

(e) 37% ENGINE SPEED, 120° RADIATION ANGLE.

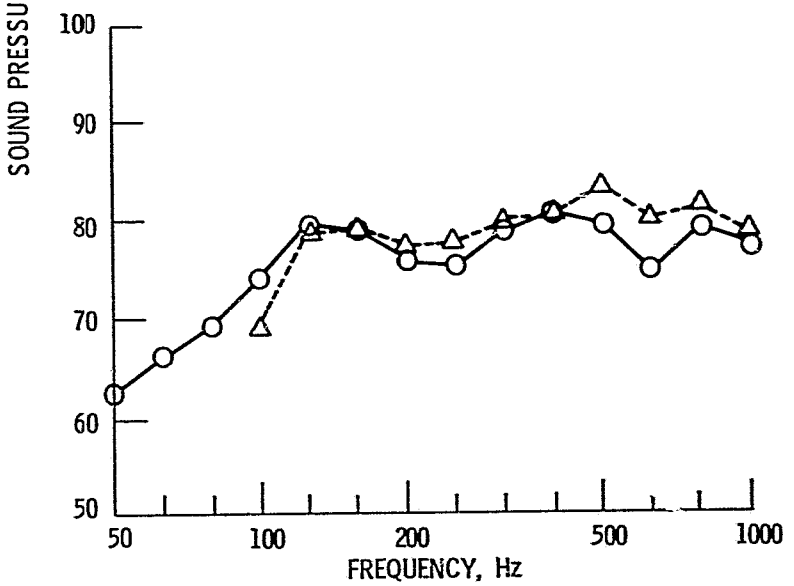

(f) 43% ENGINE SPEED, 120° RADIATION ANGLE.

Figure 12. - Concluded.

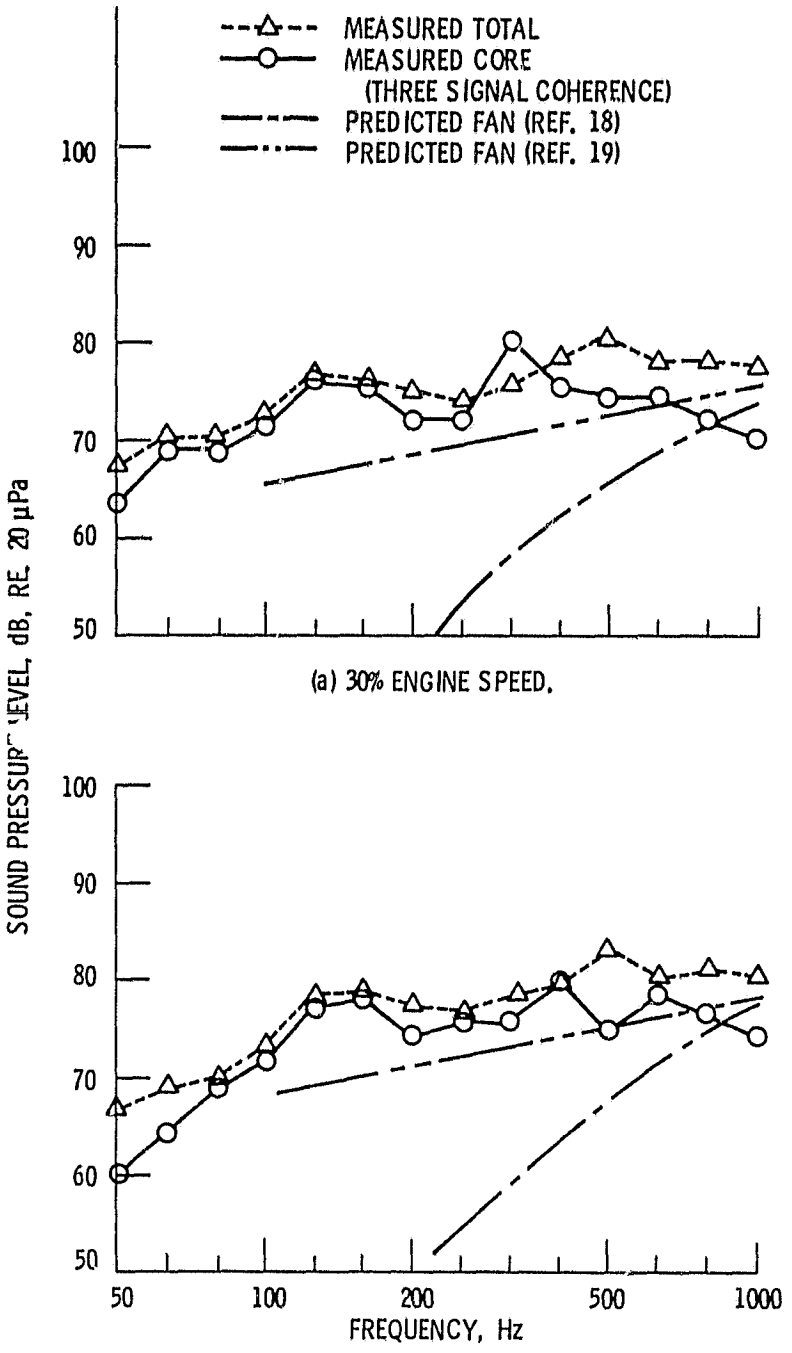

(a) 30% ENGINE SPEED.

(b) 37% ENGINE SPEED.

Figure 13. - Comparison of fan noise predictions using method of references 18 and 19 with measured core and total noise at 120^0 from engine inlet.

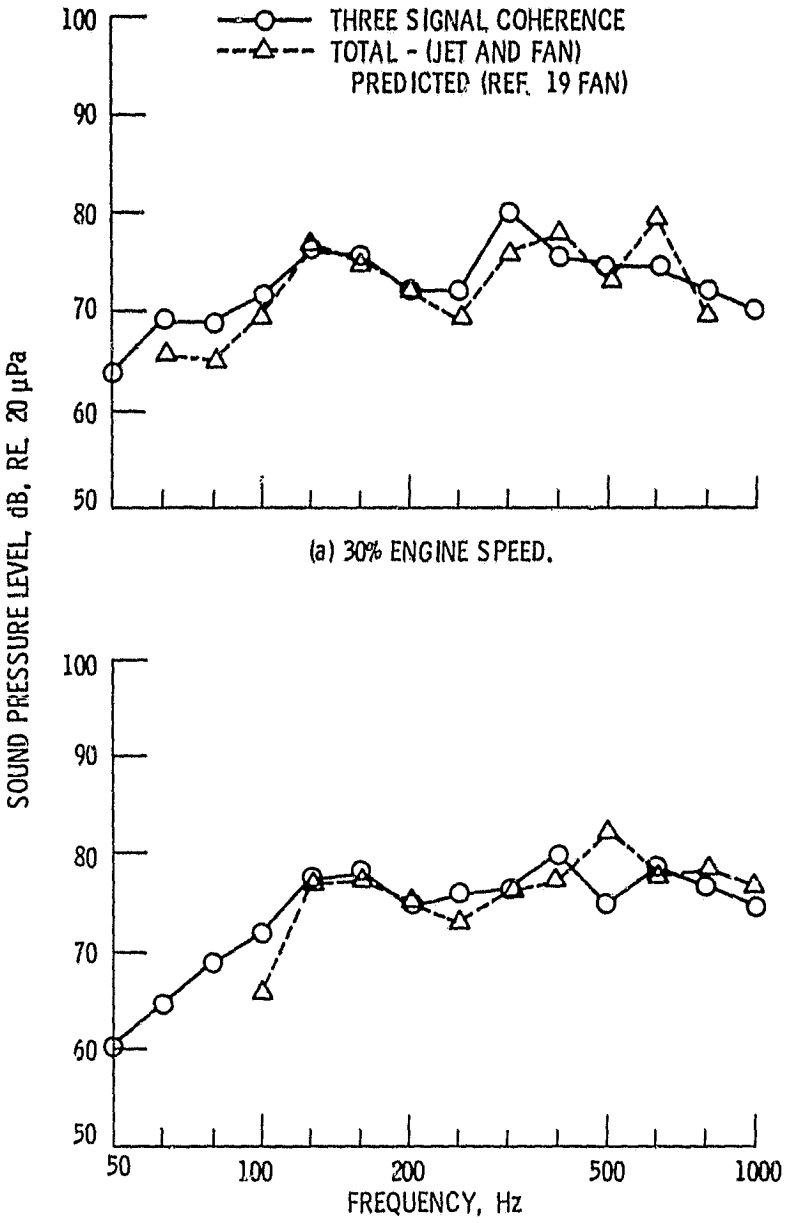

(a) 30% ENGINE SPEED.

(b) 37% ENGINE SPEED.

Figure 14. - Comparison of core noise measured using three signal coherence technique with core noise estimated by subtracting jet and fan noise from the measured total noise using reference 19 fan noise prediction, 120^0 from engine inlet.

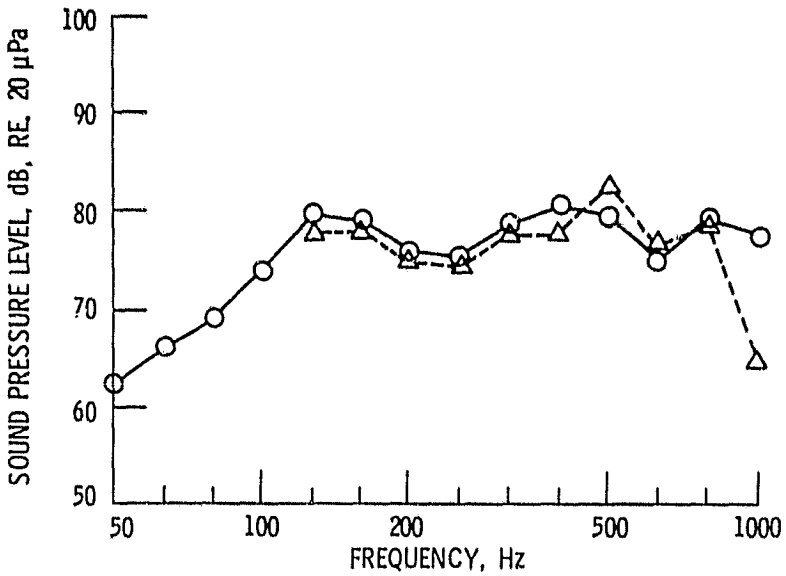

(c) 43% ENGINE SPEED.

Figure 14. - Concluded.

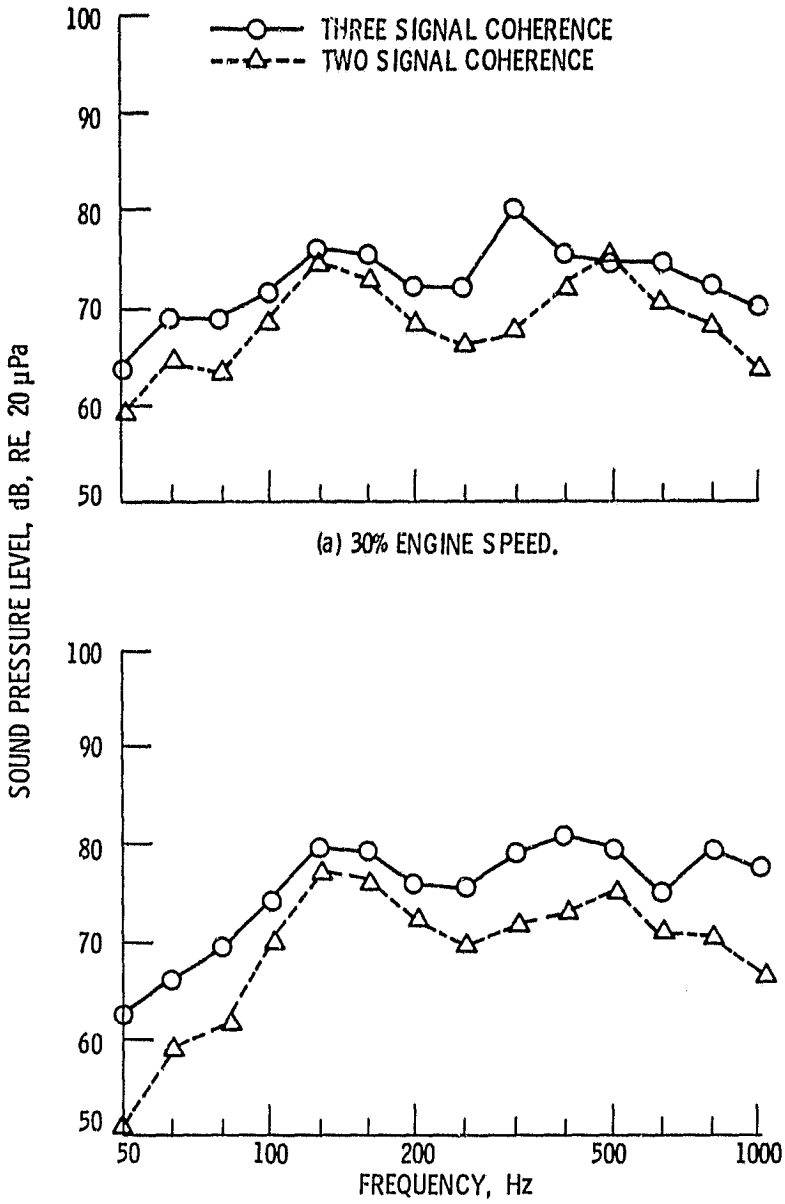

(a) 30% ENGINE SPEED.

(b) 43% ENGINE SPEED.

Figure 15. - Comparisons of core noise levels determined using three signal coherence technique with core noise levels determined using two signal coherence method, 120^{0} from engine inlet.

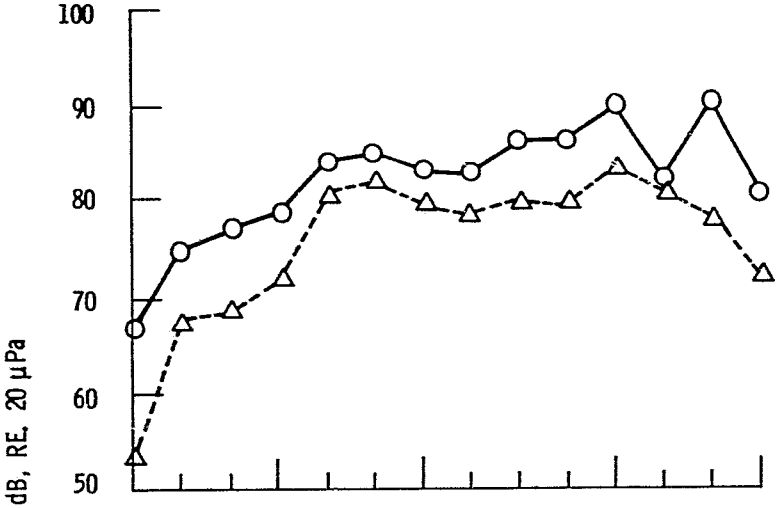

(c) 60% ENGINE SPEED.

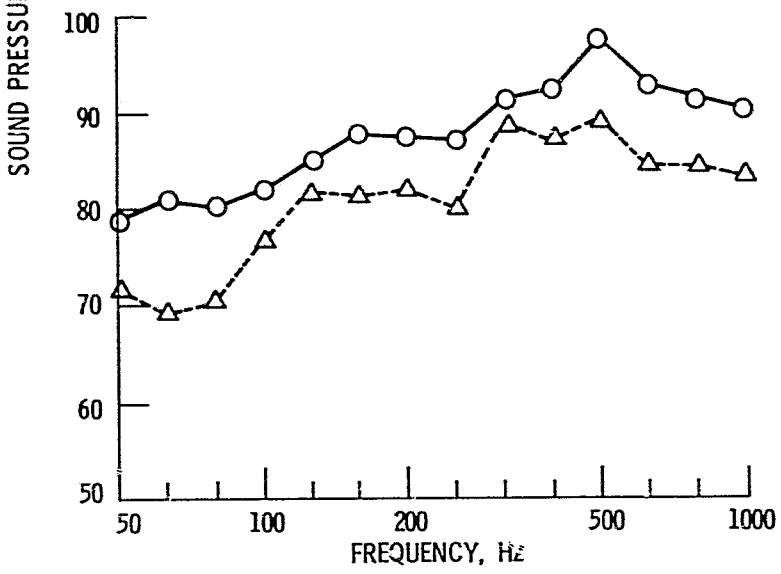

(d) 95% ENGINE SPEED.

Figure 15. – Concluded.

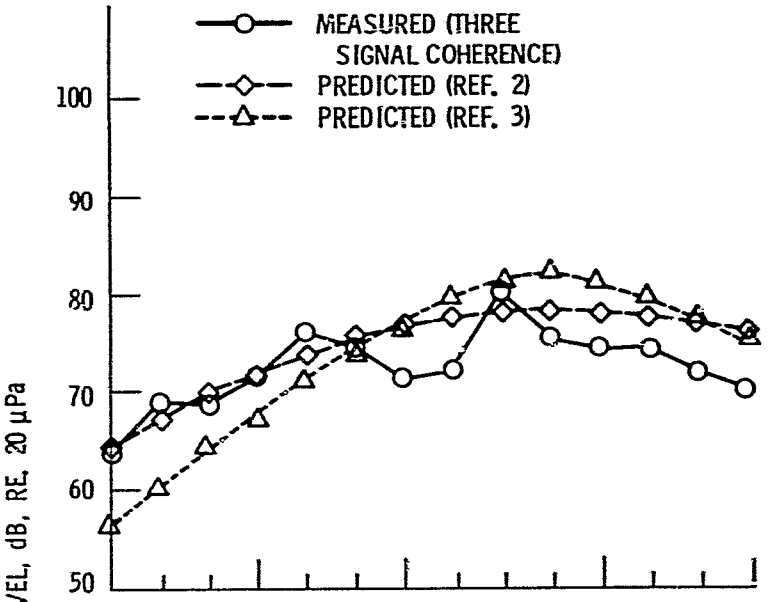

(a) 30% ENGINE SPEED.

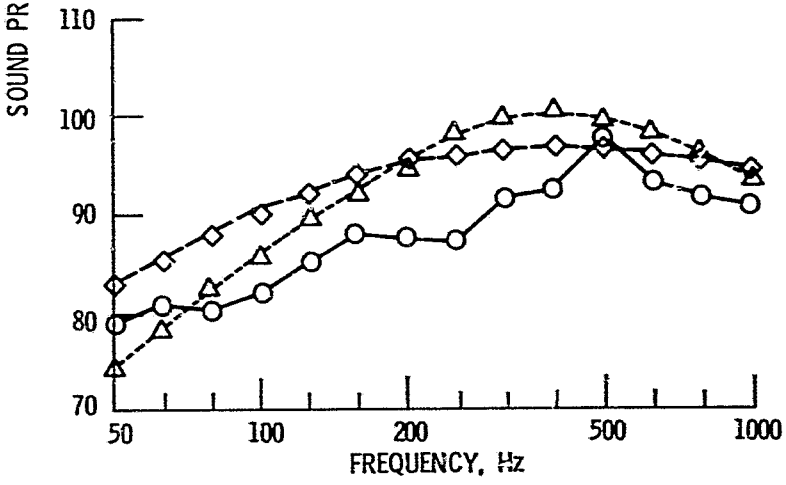

(b) 95% ENGINE SPEED.

Figure 16. – Comparison of measured and predicted core noise spectra at 120° from engine inlet.

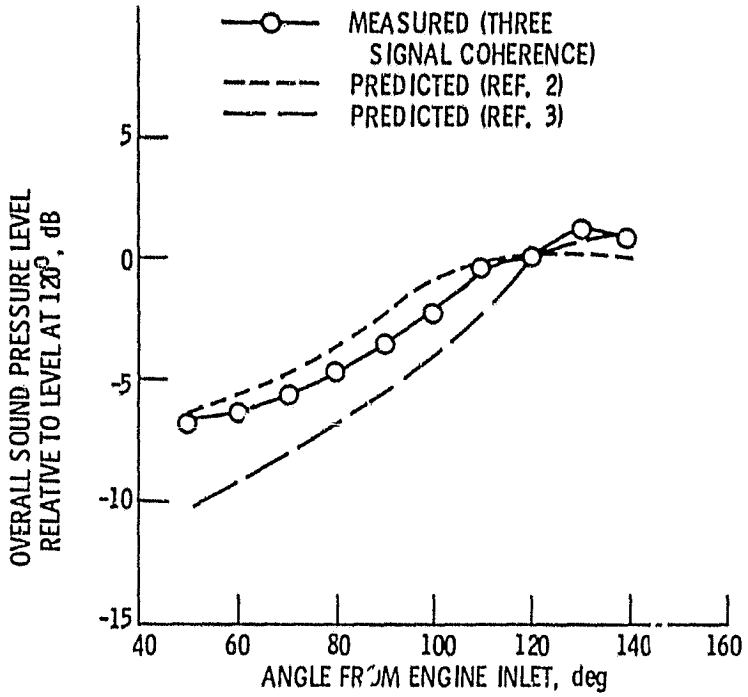

Figure 17. - Comparison of measured and predicted overall sound pressure level directivities, 30% engine speed.